25th ABCM International Congress of Mechanical Engineering
October 20-25, 2019, Uberlândia, MG, Brazil

COB-2019-0769
VORTEX INDUCED VIBRATION IN A SINGLE DEGREE OF FREEDOM CYLINDER WITH STRUCTURAL NONLINEARITIES

Sérvio Túlio Suenai Haramura Bastos
Rui Marcos Grombone de Vasconcellos
São Paulo State University (UNESP), Av. Professora. Isette Corrêa Fontão, 505, São João da Boa Vista, SP, 13876-750
e-mails tuliobastos10@gmail.com, rui.vasconcellos@unesp.br

Flávio Donizeti Marques
University of São Paulo (USP), Av. Trabalhador Sancarlense, 400, São Carlos, SP, 13566-590
e-mail fmarques@sc.usp.br

Abstract. *In this research project, it is proposed the investigation of the effects of hardening structural nonlinearity in a single degree of freedom cylinder exposed to a transverse flow, presenting the vortex induced vibration effect. To check the validity of the implemented phenomenological model, numerical simulations have been performed and the results have been compared with experiments. Simulations showed that the presence of this type of nonlinearity extends the lock-in region by changing the structural natural frequency as the amplitude of oscillations increases with the freestream speed and the vortex shedding frequency. Besides, other parameters, such as the mass and the diameter of the cylinder, affect the synchronization region. A wind tunnel test validated of the obtained simulated results. The contributions of this research can be helpful in order to prevent vortex induced vibrations in realistic nonlinear structures.*

Keywords: *Vortex induced vibration, nonlinear structures, hardening structural nonlinearity.*

1. INTRODUCTION

Structures with cylindrical shape are widely employed in engineering, for example, landing gear in aircraft, bridge pillars, chimneys, transmission lines and especially in the extraction of oil from under sea. Such pipes, known as *risers* are exposed, at certain conditions of maritime current velocity, to vibrations that can reach high amplitudes, leading to possible serious damages, including oil spills that often result in both immediate and long-term environmental damage. Thus, Vortex Induced Vibrations (VIV) modeling becomes important, both for understand, prevent and for the development of techniques to control those vibrations.

Vortex-Induced Vibration is consequence of a turbulent region created from the shedding of the boundary layer. Because of the fluid-structure interaction, vortex shedding can occur and then, periodic aerodynamic forces can excite the structure (Andrianne, 2012).

The Reynolds number is an important indicator of the type of the flow. The VIV can be occurring if this number indicates a range where the named Von Karmàn vortices occur. When this range is achieved is possible to analyze the vibration and then another number becomes important for the analyses. The Sthrouhal number rises as an indicator of vortex shedding pattern. Let the freestream speed U, the diameter D of the cylinder and the shedding frequency ω_s is possible to define the Strouhal number as:

$$S_t = (\omega_s D)/(2\pi U) \tag{1}$$

When the vortex shedding frequency is near of natural frequency there is a region of oscillations denoted as lock-in or synchronization. Because of this coupling between frequencies, large oscillatory motion can occur and this becomes a concern for several structures (Lopes, 2009).

The approach that considers only a linear structure is not sufficient to describe the reality with efficiency. Applying nonlinearities, such polynomials, the model becomes more realistic. One of the more common nonlinearities is the structural *hardening*, in which the stiffness rises with the increase of the displacement.

Therefore, main goal of this research is understand the effects of this type of nonlinearity and implement a semi-empirical model to describe this phenomenon. Besides, a wind tunnel test is performed to validate it.

2. THE THEORETICAL MODEL

A possible modeling approach to VIV was presented by Facchinetti et al. (2004), which uses the Van Der Pol oscillator model with a rigid cylinder, with diameter *D*, supported elastically and able to oscillate on a transverse uniform and stationary flow *U*, as shown in Fig 1.

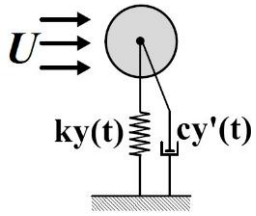

Figure 1. Conventional sketch of a VIV system. Adapted from Dai et al., 2015.

Thus, the cylinder oscillates with displacement *y* and it is described as follow:

$$my'' + cy' + k\,y = F \tag{2}$$

where, $m = m_s + m_f$ is the total mass, that is, the structure mass (m_s) and the added mass of fluid (m_f), *c* is damping coefficient, *k* is the spring stiffness and *F* is the forcing term that includes the Van Der Pol nonlinear oscillator. In order to represent realistic structures, the phenomenological model is modified to incorporate structural nonlinearities, in the case of the present research; the effects of the structural hardening nonlinearity in the vortex induced vibrations will be investigated. This type of nonlinearity is characterized by increase of the stiffness with increase of displacement. Thus, it is possible rewrite the Eq. (2) as:

$$m\,(y'' + 2\omega_0\zeta y' + G(y)\omega_0^2 y) = F(t, ...) = F[y,q(t)] \tag{3}$$

where *q(t)* is the evolution of the wake-oscillator and it can be described as:

$$q'' + \lambda\,\omega_s\,(q^2 - 1)\,q' + \omega_s^2 q = f_s \tag{4}$$

parameter λ is an empirical coefficient determined by Facchinetti et al. (2004) and f_s is the forcing term defined as:

$$f_s = P/Dy'' \tag{5}$$

being *P* an empirical coefficient determined by Facchinetti et al. (2004).

At last, the term denoted by *G(y)* is going to change the structural stiffness by including nonlinear terms as:

$$G(y) = \alpha + \beta\,y^2 \tag{6}$$

being α and β are the linear and cubic coefficients of hardening nonlinearity.

3. THE EXPERIMENTAL APPRATUS' DESCRIPTION

To build the experimental model, first it was important choose how to obtain the main effects of the structural hardening. Using the same approach used by Huynh et al. (2015), it was chosen the bilinear nonlinearity because of the facility to obtain the changing of the stiffness. Basically the bilinear nonlinearity has two linear different stiffness. Between some displacements it gives one fixed value of stiffness and from the discontinuity point the stiffness increases instantaneously and it becomes to have another value, bigger than the first, Fig 2.

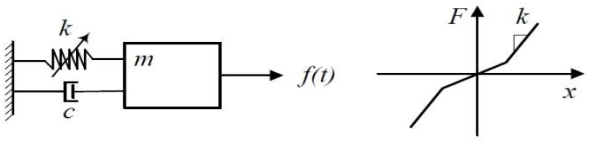

Figure 2. Mechanical system with bilinear spring to approximate the hardening effect. Adapted from Huynh et al. (2015).

The difference between the cubic hardening nonlinearity and the last one are the discontinuity points. When is analyzed the hardening stiffness, is possible to verify the hardening is continuous and the bilinear has a point of discontinuity. However, the main effect is obtained by this approximation, that is, the change and the increase of the stiffness.

After determined how to obtain the hardening effect it was possible to build the real model to use in the wind tunnel test, as presented in Fig 3.

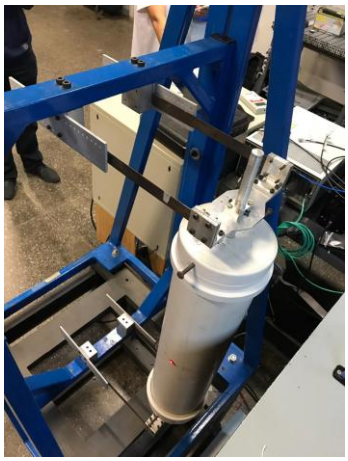

Figure 3. Experimental VIV model with structural hardening stiffness.

The experimental apparatus was constructed with a polyvinyl chloride cylinder with a central aluminum shaft supported by four crimped carbon steel beams with a length of 290mm, a thickness of 1.3mm and a width of 20.5mm, that provides the linear stiffness. Besides, the aluminum side beams with variable length provides different behaviors of structural hardening. When the side beams are completely retracted the linear case is exhibited, but by the increasing of the length the nonlinear stiffness increases and the hardening effects rises.

The amplitude measured system is composed by two accelerometers arranged on the top and bottom of the cylinder and a laser vibrometer in the middle of it. All of them were connected to a DSPACE® board. The blower wind tunnel has an opens section with a 50 x 50 cm cross section area. It is instrumented with a pitot-static air speed measure,eletronic speed controller and pressure/temperature gauges. The maximum air speed is limited to 30m/s.

4. VALIDATION OF LINEAR STRUCTURAL CASE

In order to obtain the natural frequency of the experimental device and search for possible additional modes a modal analysis was performed. Figure 4 presents a frequency domain response to impact.

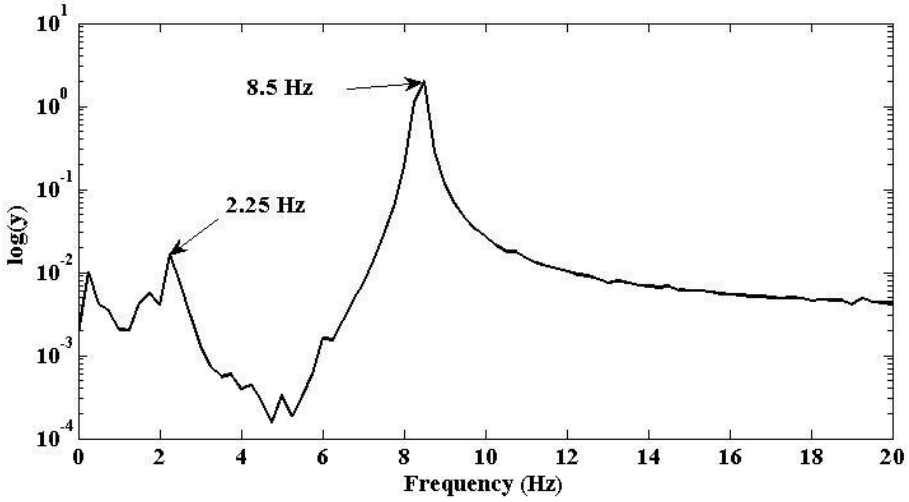

Figure 4. Principal frequencies of experimental model obtained by modal analyses.

Analyzing the Fig. 4 is possible observe the apparatus has two principal modes, the fundamental in 2.25 Hz and a second in 8.5 Hz. The physical and empirical parameters of the experimental apparatus are shown in Tab. 1.

Table 1. Physical properties and parameters of the system

Physical properties and parameters	Values
Mass, m (kg)	2.94
Diameter, D (m)	0.15
Flow density , ρ (Ar, kg/m³)	1,225
Damping coefficient, ζ	0,0005
First mode frequency (Hz)	2.25
Second mode frequency (Hz)	8.5
Empirical coefficient, λ	0,3
Empirical coefficient, P	12
Lift Coefficient, C_{L0}	0,3
Drag Coefficient, C_D	1,2

During the assembly of the experimental device and the execution of the experiments it was noted the presence of mass and stiffness asymmetries resulting in the coupling between the two modes. Thus the movement of the cylinder was the superposition of the two modes. The 2.25 Hz is related with the first mode of bending in the y direction and the 8.5 Hz, with y direction, but the opposite directions considering the top and the bottom of the cylinder.

After this, the experiment to validate the theoretical linear model was performed. Putting the experimental cylinder on the wind tunnel and varying the speed of 1m/s to 17m/s with step approximately 0.5m/s, limited by the resolution of the tunnel.

For small speeds, the cylinder had random oscillations with small amplitude, probably related with turbulence. When it was achieved 6m/s, the amplitude was regular and rose to large amplitudes. This behavior was maintained until approximately 11m/s because of the synchronization process. After this speed the amplitude decreased and the behavior of oscillation became random again until 17m/s.

Using the data of Tab. 1 in the linear model it was possible compare the theoretical results with the experiments. The comparison is presenting in Fig. 5. The theoretical model predicted the amplitude of oscillation approximately 0.41D, as well as a lock-in region between 5.5m/s and 10m/s. The experiment presented a lock-in region starting in 6m/s until 11m/s and maximum amplitude 0.4D.

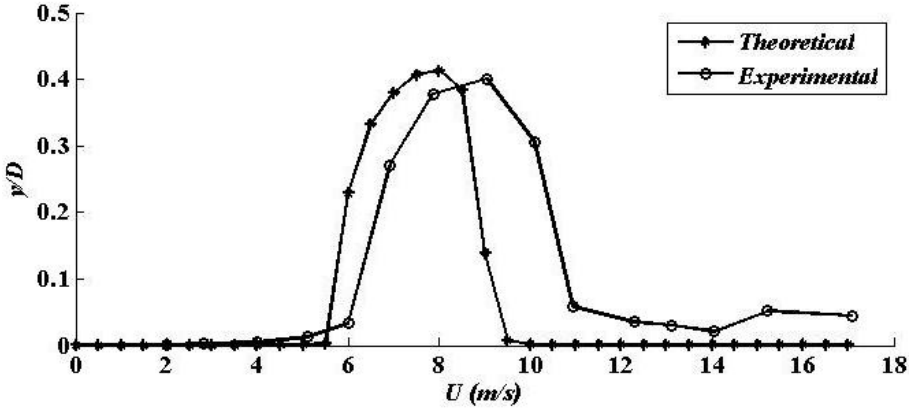

Figure 5. Comparison between theoretical model and the experiments.

Therefore, is verified that the mathematical model is in good agreement with the experiments, predicting both amplitude and synchronization region.

5. PARAMETRIC STUDY OF LINEAR MODEL

After validate the linear model it was possible to analyze what parameters have more influence in the lock-in region. All parameters have its proper influence in this region, but the mass and the diameter of the cylinder are the main parameters that affect significantly the synchronization region.

First, it was simulated two cases with the mathematical model for analyzing the mass effect keeping almost all parameters in the Tab. 1 constant, except the mass and consequently the natural frequency of the structure, the results are presented in Fig 6.

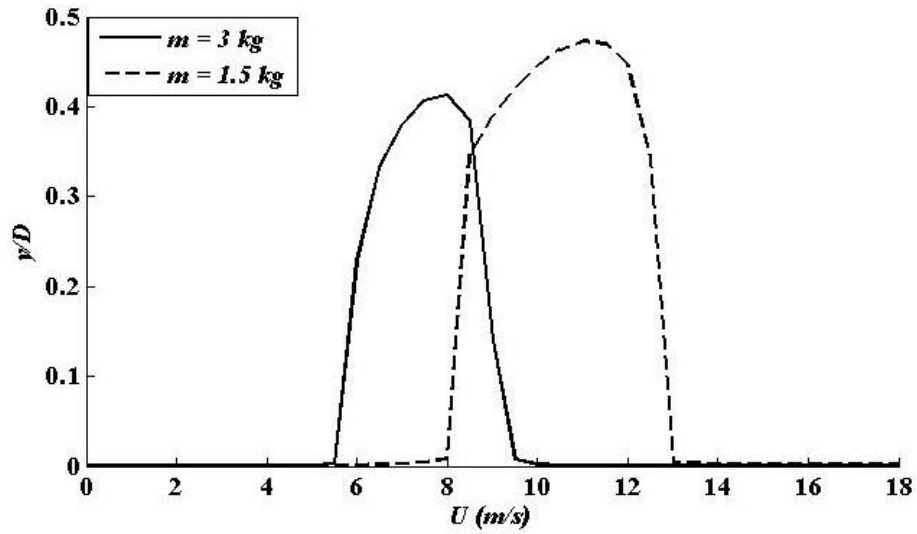

Figure 6. Effect of mass variation.

The first case is using a mass 2.94 kg, which the natural frequency is 53.4 rad/s. The mechanical system presented the lock-in region between 5.5m/s and 10m/s with maximum amplitude 0.41*D*. In the second case for a mass 1.5 kg and natural frequency 74.77 rad/s is observed a lock-in region between 8m/s and 13m/s with maximum amplitude 0.47*D*. Therefore is possible to note that the mass variation changes the structural natural frequency, if mass becomes bigger, the lock-in region is smaller and the oscillations begin earlier. Besides, increasing the mass the amplitude of oscillation decreases because inertia increases.

The influence of variation of cylinder diameter is then considered, it is noticed that when *D* increases both the amplitude of oscillation and the extension of the lock-in region increase. Keeping the other values the same of Tab. 1, it is possible obtain the results in the Fig. 7. When the diameter is 0.15m the amplitude of peak is about 0.41*D* and the range of lock-in speeds are from 5.5m/s to 10m/s. However, when it is about 0.2m the amplitude of peak is increased to 0.46*D* and the range of lock-in speeds are from 7.5m/s up to 12.5m/s.

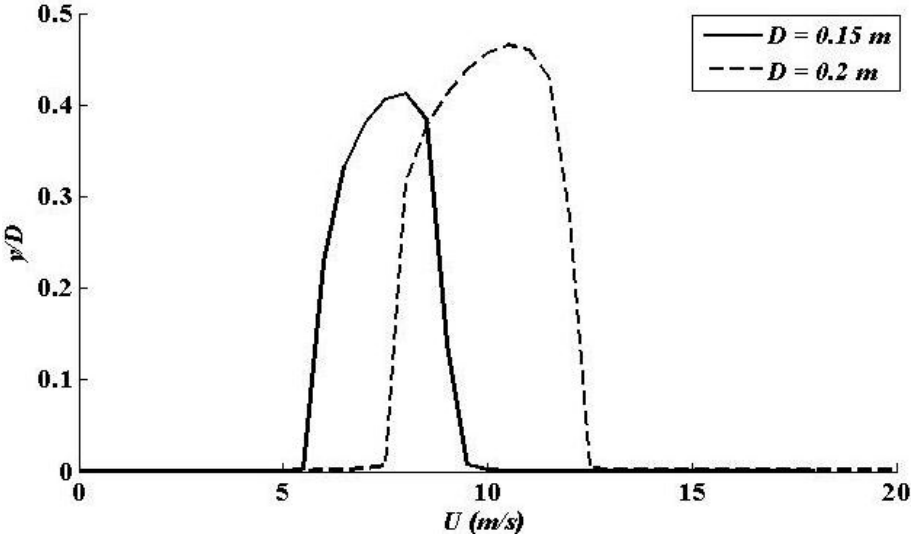

Figure 7. Diameter effect.

Therefore, the diameter variation changes the shedding frequency, if diameter becomes bigger, the lock-in region is larger and the oscillations begin later because of the shedding frequency diminishes. Besides increasing the diameter the amplitude of oscillation increases. Thus the variation of diameter and the mass have the opposite effect.

6. VALIDATION MODEL WITH STRUCTURAL HARDENING NONLINEARITY

After validate the linear model, it was started the validation of nonlinear model. Initially, the parameter α and β were determined from experiments to determinate the nonlinear stiffness. Using a laser distance meter the displacement of the cylinder, subjected to known forces.

The experimental model uses side beams which cause a bilinear hardening nonlinearity and this is approximate to cubic hardening nonlinearity, because the main behavior can be obtained, that is, the stiffness change. However polynomials functions are continuous while the bilinear nonlinearity has a discontinuity point when the stiffness changes, as shown in Fig. 8. In the real model this point is represented by the impact between the central and the side beams. After the cubic interpolation the impact effect vanishes.

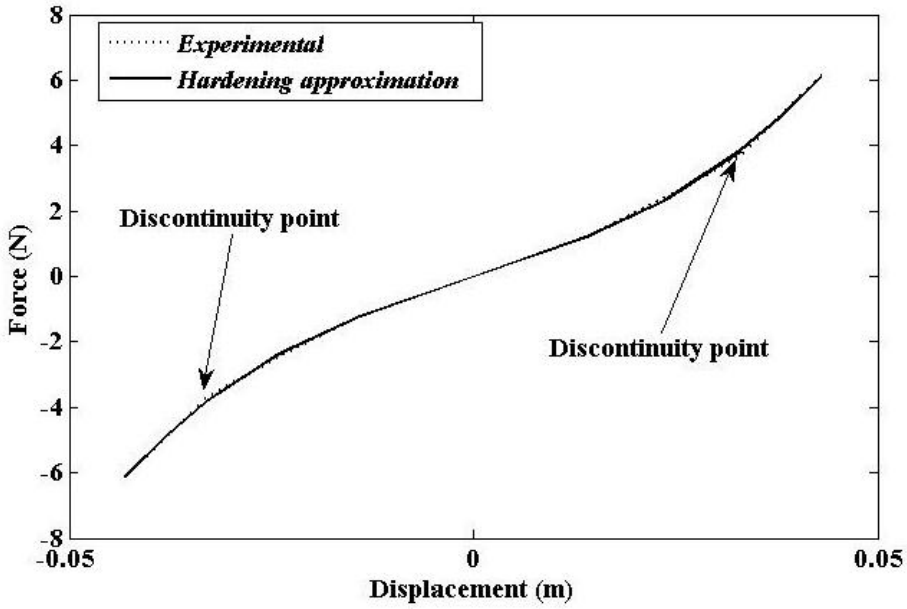

Figure 8. Comparison between experimental bilinear model and cubic approximation to β = 260.77.

Thus, it was determined the parameters to hardening stiffness. The cubic coefficient was normalized by the linear coefficient and then it was established those parameters for two different cases, as shown in Tab. 2.

Table 2. α and β parameters to nonlinear stiffness.

Linear coefficient, α	Cubic coefficient, β
1	260.77
1	491.55

Using the rigid beams to provide the nonlinear coefficient β = 260.77, it was positioned the cylinder in the wind tunnel and varied the speed from 3m/s up to 13m/s, with step approximately 0.5m/s. When the speed was small, there were random oscillations probably due to turbulence. Achieving approximately the speed 5.3m/s up to approximately 12m/s, the mechanical system presented regular oscillations with high amplitude, certainly due to the synchronization process. The contact with the side beam occurred from 5.65m/s until 12m/s. After this speed up to 13m/s, the system returned to irregular and small amplitude of oscillation.

Considering the data presented in Tab. 1 and the first configuration of Tab. 2, it was possible to simulate the situation described above. The results, using the second mode, are presenting in Fig. 8 with the experimental results. Analyzing the Fig. 9 is possible to note that the theoretical model predicted amplitude approximately 0.46*D*, as well as lock-in region between 5.5m/s and 12.5m/s. The experiment had the synchronization from 5.3m/s up to 12m/s approximately, and the maximum amplitude 0.25*D*.

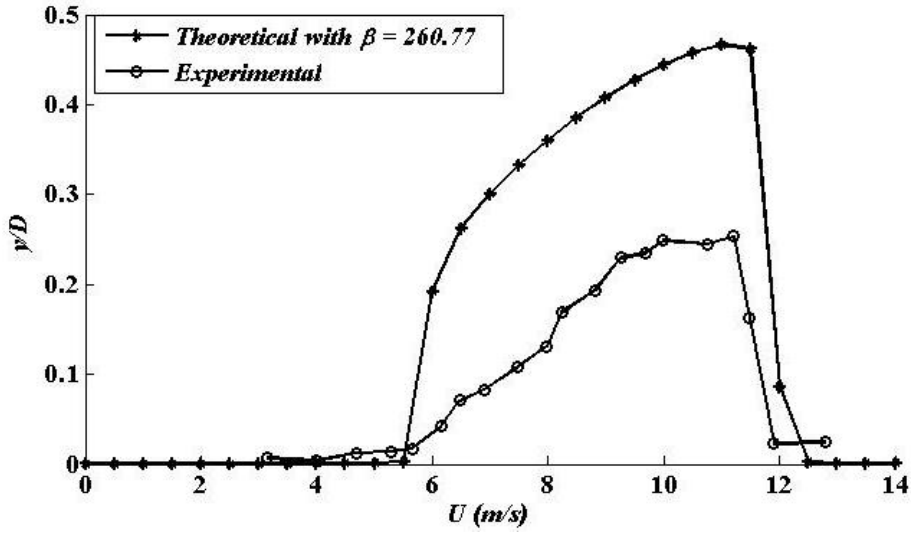

Figure 9. Comparison between theoretical model with β = 260.77 and the experiment.

Repeating the same process, but using the second configuration β = 491,55 and varying the speed approximately 5.5m/s up to 14.32m/s with step approximately 0.5m/s. From speed 5.5m/s up to approximately 14.32m/s, the mechanical system presented regular oscillations with high amplitude, certainly due to the synchronization process. The contact with the side beam occurred from all this range. After this speed the system returned to irregular and small amplitude of oscillation.

With data presented in Tab. 1 and the second configuration of Tab. 2, it was possible to simulate the situation described above. The results, using the second mode, are presenting in Fig. 10 with the experimental results. Analyzing the Fig. 10 is possible to note that the theoretical model predicted amplitude approximately 0.49*D*, as well as lock-in region between 5.5m/s and 15m/s. The experiment had the synchronization from 5.5m/s up to 14.32m/s approximately, and the maximum amplitude 0.14*D*.

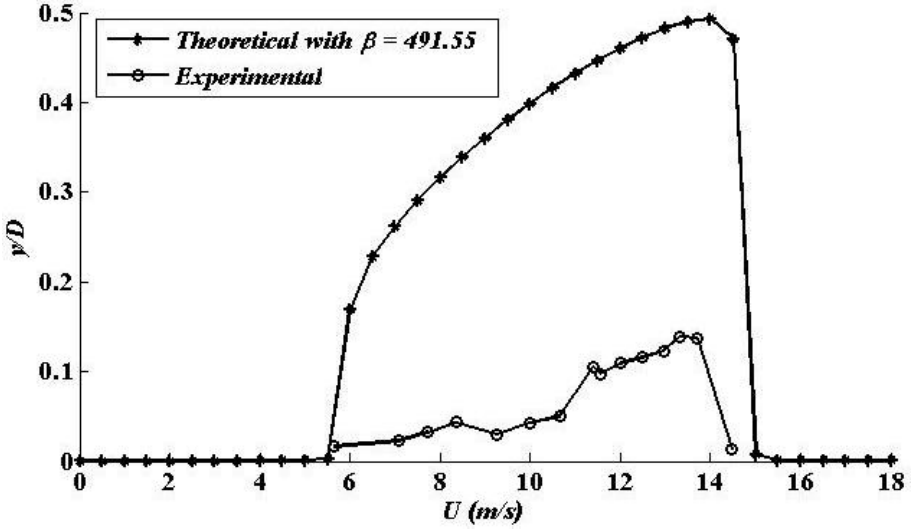

Figure 10. Comparison between theoretical model with β = 491.55 and the experiment.

Thus the mathematical model predicted the lock-in region effectively for two cases. Additionally, is verified the presence of hardening nonlinearity extends the lock-in region up to higher speeds. Additionally increasing the intensity of the cubic term extends the synchronization region, the maximum speed increased from 12 m/s with β = 260.77 to 14.32m/s with β = 491.55.

Is verified, in the both cases above, the mathematical model with hardening structural nonlinearity captured the effect of the extension of the lock-in region and its relation with the hardening intensity. However, the theoretical model failed to predict the amplitude of oscillation, probably due to the presence of asymmetries, additional modes of

vibration and the discontinuity provided by the impact of the system with the side beams presented by the experimental device.

7. CONCLUSIONS

A phenomenological model of vortex induced vibrations in a single degree of freedom cylinder under transversal flow, based on Van Der Pol oscillator was validated for linear structural stiffness and then, modified to incorporate structural nonlinearity of hardening type. Simulations to identify the influence of parameters such as mass, cylinder diameter and hardening intensity were performed. It was observed that increasing the mass of cylinder results in an anticipation of the lock-in region, also, it was noticed that the speed range in which the system present oscillations is smaller. An opposite effect is observed with the variation of the cylinder diameter, by increasing the cylinder diameter, the synchronization region starts at higher speed and the range of lock-in region is increased.

An important effect was observed when the intensity of the nonlinear structural hardening effect varies. It was shown how the variation of stiffness due to structural nonlinear hardening effect influence both the amplitude of oscillation and the lock-in speed range. As the natural frequency is function of amplitude of oscillations when hardening nonlinearity is present, as speed increase, the coupling between structure natural frequency and the vortex shedding frequency will remain for a wider range of speeds, in other words, the lock-in region can be extended if a hardening effect is present in the structure.

Although both the linear model and nonlinear model with hardening approximation were validated for lock-in region, only the linear model could predict the amplitude of oscillation. The difference of amplitude can be explained by the approximation of nonlinearity. It does not predict discontinuity provided by the impact of the system with the side beams. Moreover the theoretical model does not predict the presence of additional modes of vibration presented by the real model because the asymmetries.

The overall results reveal that the mathematical model was able to capture the main effect of the hardening structural nonlinearity, the extension of the synchronization region and its relation with the hardening intensity. Modifications in the mathematical model and in the experimental device are planned for the continuity of this research, to better understand and predict all observed effects in the experiments.

8. ACKNOWLEDGEMENTS

The authors acknowledge the financial support of the Brazilian agencies, grant 2018/00318-4, São Paulo Research Foundation (FAPESP) and CNPq (grant 311082/2016-5).

9. REFERENCES

Andrianne, T., 2012. *Experimental and numerical investigations of the aeroelastic stability of bluff structures.* Ph.D. thesis, FSA, ULiège, Liège, Belgium. [Online]. Available: https://orbi.uliege.be/handle/2268/112748

Dai, H.L., Abdelkefi, A., Wang, L. and Liu, W.B., 2015. "Time-delay feedback controller for amplitude reduction in vortex-induced vibrations". *Nonlinear Dynamics.*, Vol. 80, No. 1-2, pp. 59-70. [Online]. Available: https://link.springer.com/article/10.1007/s11071-014-1851-x

Facchinetti, M.L., Langre, E. and Biolley, F., 2004. "Coupling of structure and wake oscillators in vortex-induced vibrations". *Journal of Fluids Structures*, Vol. 19, No. 2, pp. 123-140. [Online]. Available: https://reader.elsevier.com/reader/sd/pii/S0889974603001853?token=039523BB3A9F3F1B5D1D65F4447CFB32C481092B752929F62234C9D4147945DE59DD38FCE739B6093BA74B32C9F8033C

Huynh, B.H., Tjahjowidodo, T., Zhong, Z.W., Wang, Y. and Srikanth, N., 2015. "Nonlinearly enhanced vortex induced vibrations for energy harvesting". In *2015 IEEE International Conference Advanced Intelligent Mechatronics*, Busan, South Korea, pp. 91-96. [Online]. Available: https://ieeexplore.ieee.org/stamp/stamp.jsp?tp=&arnumber=7222514

Lopes, R.K.D., 2006. *Análise de estruturas sujeitas a vibrações induzidas por vórtice.* M.S. thesis, COPPE, UFRJ, Rio de Janeiro, Brazil. [Online]. Available: http://www.coc.ufrj.br/es/documents2/mestrado/2006-1/1615-rita-de-kassia-dias-lopes-mestrado/file

10. RESPONSIBILITY NOTICE

The authors are the only responsible for the printed material included in this paper.